Automatic Detection of the Number of Raypaths in a Shallow-Water Waveguide

Longyu Jiang, Jerome I. Mars

Automatic Detection of the Number of Raypaths in a Shallow-Water Waveguide

Longyu Jiang and Jérôme I. Mars *Member, IEEE*

Abstract

Correct identification and tracking of stable raypaths are critical for shallow-water acoustic tomography. According, separating raypaths using high resolution methods is presented to improve resolution ability based on the prior knowledge of the number of raypaths. It is clear that the precise knowledge of the number of raypaths largely determines the separation performance. Therefore, a noise -whitening exponential fitting test (NWEFT) using short-length samples is proposed in this paper to automatically detect the number of raypaths in a shallow-water waveguide. Two information theoretic criteria are introduced as comparative methods. Their performances are tested with simulation data and real data obtained at small scale. The experimental results show that the noise-whitening exponential fitting test can provide satisfactory detection compared to the two classic information theoretic criteria — the Akaike information criterion (AIC) and the minimum description length (MDL). Referring to the performance of AIC and MDL, MDL is asymptotically consistent while AIC overestimates even if analyzed asymptotically.

Index Terms

Array signal processing, Akaike information criterion (AIC), minimum description length (MDL), noise whitening exponential fitting test (NWEFT), shallow-water tomography.

I. Introduction

Shallow water refers to the region from the end of the surf zone out to the continental shelf break. It is an environment differing from deep water. The principal motivation of shallow-water research comes from the significant contributions to naval defense issues, to biology, to geology,

Longyu Jiang and Jérôme I. Mars are with the Department of Signal and Image Processing, Gipsa-lab, Grenoble Institute of Technology, Grenoble, 38402, France. e-mail: (Long-Yu.Jiang@gipsa-lab.grenoble-inp.fr).

and to physical oceanography. Moreover, easier measurements of the environment parameters at smaller scale are achieved as seen for bathymetry and the sound-speed fluctuations. Simpler array deployments are also merits of shallow water due to the shorter array lengths. On the other hand, acoustic tomography is explored to image the sound-speed variations of the ocean interior. It was first introduced as a remote-sensing technique in deep water using low-frequency sound for the large-scale of the ocean [1]. However, acoustic tomography in shallow-water has been paid more attention in recent studies [2] [3] [4] [5] [6] for the motivation and merits introduced before.

Specifically, a briefing of ocean acoustic tomography process is described as: the broad acoustic signals are primarily emitted by a point source. Then, transmitting broad band pulses in the ocean lead to a set of impulsive arrivals at the receiver which characterize the impulse responses of the sound channel. The peaks observed at the receiver are assumed to represent the arrival of energy traveling along geometric raypaths. Acoustic propagation with higher frequencies in shallow water can be considered as parallel propagation in deep water due to wavelength scaling. A common way to proceed is to take advantage of the multi-path properties of the wavefield. Each raypath can provide information on the variation of the sound distribution. Nevertheless, multi-path propagation not only provides more information but it also produces interferences between raypaths. Furthermore, it is not possible to obtain satisfying tomography results if the number of separated raypaths is too small. Thus, ray extraction which refers to the need that the sound pulse corresponding to each raypath to be parted is defined as the forward problem of the OAT.

There are numerous approaches to source localization and geo-acoustic inversion as well as acoustic tomography relies on accurate raypath extraction in underwater acoustics. For instance, a geo-acoustic inversion method was recently reported in [7]. This method estimates range-dependent geo-acoustic properties by using the relative travel-time and magnitude measurements of the most significant raypaths. To improve the efficiency of the inversion process, automatic identification of signal raypaths was developed [7]. A demonstration of these algorithms is given in [8] with broad-band data from a real experiment during the Shallow Water 2006 experiments. Concerning source localization, in [9] and [10], a Gibbs sampling-maximum a-posteriori estimator is presented to estimate time delays and amplitudes of arrivals. Bypassing computationally demanding analysis, Gibbs sampling is proposed as an efficient means for estimating the necessary posterior probability distributions.

To extract more raypaths in the context of ocean acoustic tomography, beamforming has been considered in a point to array configuration. Although benefits of using beamforming in such configuration have been reported in [1], its major drawback is the limited resolving ability. To improve the resolution of beamforming, a novel configuration composed of a vertical array of sources and a vertical array of receivers (i. e. an array to array configuration) was proposed in [3] [4]. The source array provides the emitted angle as an additional discrimination parameter to separate more raypaths. However, this is still confronted with the disadvantage of low resolution performance. As a first step of improvement, a smoothing-MUSICAL (MUSIC Active Large-band) method which is a combination of MUSICAL and spatial-frequency smoothing has been developed for extracting observations in the context of ocean acoustic tomography [11]. It turns out that smoothing-MUSICAL achieves better separation and stronger robustness than beamforming; nevertheless, as one of subspace-based methods, the separation using smoothing-MUSICAL also requires the correct prior knowledge of the number of rayspaths. Poor selection of the number of rayspaths would lead to hampered separation.

To determine the subspace dimension, two commonly suggested approaches are the Akaike information criterion (AIC) and the minimum description length (MDL) [12]. In [13] and [14], MDL has been obtained based on coding arguments and the minimum description length **(MDL)** principle while in [15] and [16], the same rule is derived in a Bayesian framework. Both of AIC and MDL consist of minimizing the Kullback-Leibler discrepancy between the probability density function of the data and the probability density function of the model. With ideal assumptions of ergodic Gaussian random processes, the MDL criterion is shown to be asymptotically consistent, whereas the AIC tends to overestimate the order of the model. In contrast, these ideal assumptions may not be fulfilled in practice and several factors can result in the smallest eigenvalues being dispersed (e. g., reduction in the number of samples or low SNR). Both the AIC and the MDL tend to overestimate or underestimate the order of the model. For the analysis of the performance and evaluation of the probability of over or under estimation of the AIC and MDL, theoretical and simulation results have been presented [17] [18]. In addition, MDL-based processor which exploits an order statistics approach in the existing solution has been constructed by Fishler and Messer [19]. This new processor improved the performance at the price of greater complexity. Moreover, Valaee and Kabal [20] proposed a novel information theoretic algorithm to estimate the number of signals for coherent signals in array processing. Differing from the MDL, it defined

the predictive description length (PDL) criterion as the length of a predictive code for the set of observations. The PDL criterion is computed for the candidate models and is minimized over all models to select the best model and to determine the number of coherent as well as noncoherent signals. The simulation results show that the performance of the PDL algorithm is better than that of the MDL. Practically, a Bayesian information criterion which is needed to sufficiently fit the data while satisfying parsimony to avoid overparametrization is exploited to decide on the number of sediment layers in the background of performing inversion of seabed reflection data. [21]. Two alternative Bayesian methods were also proposed by Djuric [22] [23]. In [23], maximum a posterior (MAP) rules that has the similar forms as AIC and MDL are developed for different families of competing models based on their inference that the penalty term has to vary in the model structure and type of model parameters. By considering the penalty variation which is in type of model parameters, a model selection criterion is derived by weighting penalties associated with the amplitude and phase parameters differently than the one attached to the frequencies in [22].

Another group of methods is the likelihood ratio test [24] [25] [26], which is performed by direct minimized the Kullback-Leibler of the probability density function of the model. For example, the nested likelihood ratios [26] are shown to be asymptotically independent and sufficient for estimating the number of signals and to implement resolutions of superimposed signals into individual signals. It has been shown that a natural implementation of the information criterion is a more straightforward way of implementing the generalized likelihood ratio test with a specific threshold [27].

By first considering the observation limitations, a test for the determination of the dimension of a signal subspace from short data records was explored by Shah and Tufts [28]. This consisted of the interpretation of the sum of squares of singular values as energy in a particular subspace. The constant false alarm rate thresholds were set up based on distributions derived from matrix perturbation ideas. It is worth noting that a criterion based on eigenvalue ratios can be used to look for an eigenvalue gap between the noise and the signal eigenvalues [18]. As a following method, a test that exploits the exponential profile of the ordered noise eigenvalue, which was originally introduced in [29], is developed to estimate the number of significant targets in time-reversal imaging [30]. Also, for estimating the number of high-dimensional signals, a sample-eigenvalue-based procedure using relatively few samples has been presented [31]. This could

consistently detect the number of signals in white noise when the number of sensors was less than the number of signals.

As a long duration of the received signals in the context of ocean acoustic tomography is not available, an exponential fitting test (EFT) using short-length samples is proposed to determine the number of raypaths in the following part, which would be considered robust and acceptable. We define short-length samples as the concept that the number of samples is equal to the number of sensors.

This paper is organized as follows: In Section II, we state the problem of detecting the number of ray paths. Then, two information theoretic criteria are introduced as comparative methods in the Part A of Section III. The EFT is specifically developed in the Part B of Section III. We show the results of a simulation to illustrate its performance in Section IV. Furthermore, the proposed test is applied to real data in Section V, which was obtained in a small-scale environment. Meanwhile, a whitening noise process is used as a preprocessing step because of considering the existence of colored noise. Section VII provides the conclusion and the future direction of our studies.

II. The Problem of Detection of the Number of Raypaths

To analyze the problem of efficient detection of the number of raypaths, the suitable model should be built first. In this paper, the model is built on an acoustic field composed of p raypaths on a vertical array of M sensors ($p < M$). The temporal signal received on the sensors is modeled as:

$$\mathbf{x}(t) = \mathbf{y}(t) + \mathbf{n}(t) = \mathbf{A}e(t) + \mathbf{n}(t) = \sum_{j=1}^{p} \mathbf{a}(\theta_j)e(t) + \mathbf{n}(t) \tag{1}$$

With:

- $\mathbf{x}(t)$: a $M \times 1$ observation vector. The ith component is the received signal on the ith sensor.
- $\mathbf{y}(t)$: the noiseless observation vector of size $M \times 1$, which spans the signal space generated by the steering vectors.
- $\mathbf{n}(t)$: additive white Gaussian noise of size $M \times 1$ with distribution $\mathcal{N}(0, \sigma^2\mathbf{I})$, which is assumed not to be correlated with the signals.
- $\mathbf{A}$: the matrix of the p steering vectors. Each steering vector $\mathbf{a}(\theta_j)$ for the j th raypath is generally characterized by the parameters of the arrival angles θ_j.

- $e(t)$: the emitted signal.

Based on (1), the observation covariance matrix $\mathbf{R}_x$ is written as:

$$\mathbf{R}_x = E[\mathbf{x}(t)\mathbf{x}^H(t)] = \mathbf{R}_y + \mathbf{R}_n = \mathbf{A}\mathbf{R}_e\mathbf{A}^H + \sigma^2\mathbf{I} \tag{2}$$

With

- R_y is the covariance matrix of $\mathbf{y}(t)$.
- R_n is the noise covariance matrix.
- R_e is the covariance matrix of $e(t)$, and H denotes the conjugate transpose.

The matrix A is assumed to be of full column rank, and R_e is nonsingular. The rank of $\mathbf{R}_y$ equals the number of raypaths p. That is, there exists p nonzero eigenvalues which correspond to the raypaths. In the same way, the smallest $M - p$ eigenvalues of $\mathbf{R}_y$ are equal to zero. Therefore, if the eigenvalues of $\mathbf{R}_x$ are arranged in descending order as $\lambda_1 \geq \lambda_2 \cdots \geq \lambda_p$, the value of the smallest $p - q$ eigenvalues which correspond to the noise is:

$$\lambda_{p+1} = \lambda_{p+2} = \cdots = \lambda_M = \sigma^2 \tag{3}$$

Hence, it is not difficult to determine p from the multiplicity of the smallest eigenvalue of $\mathbf{R}_x$. However, in practice, $\mathbf{R}_x$ is unknown. It is generally estimated by the sample covariance matrix:

$$\hat{\mathbf{R}}_x = \frac{1}{N}\sum_{t=1}^{N}\mathbf{x}(t)\mathbf{x}^H(t) \tag{4}$$

Where N is the number of samples. As $\hat{\mathbf{R}}_x$ is computed from a finite number of samples, the smallest $p - q$ eigenvalues are no longer equal to each other and σ^2 with probability one. Thus, in most cases the number of raypaths can not be determined directly by the above method.

III. Techniques for detection of the number of Raypaths

A. Information theoretic criteria

As noted in Section I, several methods have been studied for the correct detection of the number of signals. It is known that two commonly suggested methods, an information theoretic criterion suggested by Akaike (AIC) [13] [32], and the minimum description length (MDL) proposed by Schwartz [33] and Rissanen [34], can be used for model selection. Wax and Kailath [12] take the detection problem as a model selection problem and propose the following formulas for the detection of the number of signals received by a sensor array:

1) The Akaike information criterion:

$$\widehat{p} = arg \quad min_{k\in 0,1,...,M-1} \left\{ -log(\frac{g(k)}{a(k)})^{N(M-k)} + k(2M-k) \right\} \tag{5}$$

The first term in the brackets is computed from the log-likelihood of the maximum likelihood estimator of the parameters of the model. The second term is a bias correction term to make the AIC an unbiased estimate of the mean Kulback-Liebler distance between the modeled density and the estimated density. $a(k)$ and $g(k)$ are the geometric mean and arithmetic mean of the smallest $M-k$ eigenvalues respectively, which are denoted by (6) and (7). k is the number of free parameters that specifies a family of probability density functions, and $(\widehat{\lambda}_1 \geq \widehat{\lambda}_2 \cdots \geq \widehat{\lambda}_M)$ are eigenvalues generated by sample covariance matrix $\hat{\mathbf{R}}_x$ in (4). The number of raypaths $\widehat{p}$ can be estimated as the value of $k \in 0, 1, ..., p-1$, for which the AIC is minimized.

$$a(k) = \frac{1}{M-k} \sum_{i=k+1}^{M} \widehat{\lambda}_i \tag{6}$$

$$g(k) = (\prod_{i=k+1}^{M} \widehat{\lambda}_i)^{\frac{1}{M-k}} \tag{7}$$

2) The minimum description length: Although Schwartz [33] and Rissanen [34] solved the order selection problem respectively based on Bayesian and information theoretic arguments, it is highlighted that in the large-sample limit both methods get the same formulation. (8) is quite similar to the formulation of the AIC except that the correction term is multiplied by $\frac{1}{2}logN$. MDL is also performed by a recursive process for $k \in 0, 1, ..., p-1$. The k which leads to the minimum MDL value is taken as the estimated number of raypaths p.

$$\widehat{p} = arg \quad min_{k\in 0,1,...,M-1} \left\{ -log(\frac{g(k)}{a(k)})^{N(M-k)} + \frac{1}{2}k(2M-k)logN \right\} \tag{8}$$

With regard to the performance of these two methods, the MDL criterion is asymptotically consistent, whereas the AIC tends to overestimate [12]. Actually, they have the same problem as we estimate the sample covariance matrix $\hat{\mathbf{R}}_x$ directly: the number of samples is finite in practice.

B. The exponential fitting test

It is necessary to propose a method that considers the finite number of samples in view of practical limitations. For this reason, a test using an analytic expression of the ordered noise eigenvalues profiles is introduced in this section.

1) Eigenvalue profile under noise only assumption: To establish the mean profile of the decreasing noise eigenvalues, we need to calculate the expectation of each eigenvalue. For the zero-mean white Gaussian noise with power σ^2, the sample covariance matrix has a Wishart distribution with N degrees of freedom. It is a multivariate generalization of χ^2 distributions and it depends on M, N, and σ^2. In this case, the joint probability of the ordered eigenvalues shown by (9) and the distributions of each eigenvalue are given in [35] [36] as zonal polynomials, which are a multivariate symmetric homogeneous polynomials, and a fundamental tool in statistics and multivariate analysis [15] [16] as well as in random matrix theory [14]. However, the calculation of the expectation of each eigenvalue from the joint probability shown by (9) and the distribution of each eigenvalue using zonal polynomials is computationally unwieldy and gives intractable results for the moment.

$$\rho(\lambda_1,\ldots,\lambda_M) = \alpha\ exp\left(-\frac{1}{2\sigma^2}\sum_{i=1}^{M}\lambda_i\right)\left(\prod_{i=1}^{M}\lambda_i\right)^{\frac{1}{2}(N-M-1)}\prod_{i>j}(\lambda_j-\lambda_i) \tag{9}$$

As a result, we use an alternative approach to approximate the mean profile of ordered noise eigenvalue with the help of the first and second order moments of the eigenvalues.

From simulation results, it turns out that an exponential law is a good approximation to the mean profile of ordered noise eigenvalues. One result as the illustration for $M = 15$ shown in Figure. 1. which shows eight realizations for the cases of $N = 15$ and $N = 1025$ respectively. Mathematically, the exponential law can be defined as (10) with the first noise eigenvalue λ_1 and the exponential function r.

$$\lambda_i = \lambda_1 r_{M,N}^{i-1}, \quad i \in 2,\ldots M \tag{10}$$

To determine λ_1 and r, we consider the first and second moments of the trace of the error of the noise covariance matrix $\mathbf{\Psi}$, where $\mathbf{\Psi}$ is defined by (11).

$$\mathbf{\Psi} = \hat{\mathbf{R}}_n - \mathbf{R}_n = \hat{\mathbf{R}}_n - \sigma^2\mathbf{I} \tag{11}$$

Given that $E(tr[\mathbf{\Psi}_{ij}]) = 0$, we obtain (12) :

$$M\sigma^2 = \sum_{i=1}^{M} \lambda_i \tag{12}$$

According to the definition of the error covariance matrix, the element Ψ_{ij} of $\mathbf{\Psi}$ is expressed as:

$$\Psi_{ij} = \frac{1}{N} \sum_{i=1}^{N} n_i(t) n_j^*(t) - \sigma^2 \delta_{ij} \tag{13}$$

Consequently, $E[\|\Psi_{ij}\|^2]$ can be computed as follows:

$$\begin{aligned} E\left[\|\Psi_{ij}\|^2\right] &= E\left[\left\|\frac{1}{N}\sum_{i=1}^{N} n_i(t)n_j^*(t) - \sigma^2\delta_{ij}\right\|^2\right] \\ &= E\left[\left\|\frac{1}{N}\sum_{i=1}^{N} n_i(t)n_j^*(t)\right\|^2\right] + E\left[\left\|\sigma^2\delta_{ij}\right\|^2\right] \\ &\quad + E\left[-2\Re\left\{\sigma^2\delta_{ij}\frac{1}{N}\sum_{i=1}^{N} n_i(t)n_j^*(t)\right\}\right] \end{aligned} \tag{14}$$

Where $\Re$ represents the real part of a complex value. Each term in (14) can be computed individually:

$$E\left[\left\|\frac{1}{N}\sum_{i=1}^{N} n_i(t)n_j^*(t)\right\|^2\right] = \frac{1}{N^2}N\sigma^4 = \frac{1}{N}\sigma^4$$

$$E\left[\left\|\sigma^2\delta_{ij}\right\|^2\right] = \sigma^4\delta_{ij}$$

$$E\left[-2\Re\left\{\sigma^2\delta_{ij}\frac{1}{N}\sum_{i=1}^{N} n_i(t)n_j^*(t)\right\}\right]$$

$$= -\frac{2\sigma^2\delta_{ij}}{N}E\left[\Re\left\{\sum_{i=1}^{N} n_i(t)n_j^*(t)\right\}\right]$$

$$= -\frac{2\sigma^2\delta_{ij}}{N}\left(\frac{N\sigma^2}{2}\right) = -\sigma^4\delta_{ij}$$

Finally,

$$E\left[\|\Psi_{ij}\|^2\right] = \frac{1}{N}\sigma^4 + \sigma^4\delta_{ij} - \sigma^4\delta_{ij} = \frac{1}{N}\sigma^4 \tag{15}$$

Since the trace of a matrix remains unchanged when the base changes, it follows that:

$$\sum_{i,j} E\left\{\|\Psi_{ij}\|^2\right\} = E(tr[\hat{\mathbf{R}}_n - \mathbf{R}_n]^2) = M^2\frac{\sigma^4}{N} \tag{16}$$

and using an approximation,

$$M^2\frac{\sigma^4}{N} = \sum_{i=1}^{M}(\lambda_i - \sigma^2)^2 \tag{17}$$

With the combination of (10) and (12), we obtain:

$$M\sigma^2 = \sum_{i=1}^{M}\lambda_1 r^{i-1} \tag{18}$$

$$\lambda_1 = MJ_M\sigma^2 \tag{19}$$

where:

$$J_M = \frac{1-r}{1-r^M} \tag{20}$$

and it can obtain that:

$$(\lambda_i - \sigma^2) = (MJr^{i-1} - 1)\sigma^2 \tag{21}$$

By combining (21) with (17), the decay rate r is obtained from the following equation:

$$\frac{M+N}{MN} = \frac{(1-r)(1+r^M)}{(1-r^M)(1+r)} \tag{22}$$

In (10), r should be an exponential function. In our study, we assume that r is equal to e^{-2a} based on two reasons. One reason is that the shape of e^{-2a} is similar to the profile of ordered noise of assumption of short length (Fig. 1. a). The other reason is that it is easier to acquire the value of a through (21) thanks to the even index. By substituting $r = e^{-2a}$, (22) becomes:

$$\frac{Mtanh(a) - tanh(a)}{Mtanh(Ma)} = \frac{1}{N} \tag{23}$$

where tanh is the hyperbolic tangent function, given by:

$$tanh(a) = \frac{\sinh(a)}{\cosh(a)} = \frac{e^{2a}-1}{e^{2a}+1} \tag{24}$$

The 4th order Taylor series expression of tanh(a) is written as follows,

$$tanh(a) = a - \frac{a^3}{3} + \frac{2a^5}{15} \tag{25}$$

Inserting (25) in (23), the following biquadratic equation is produced:

$$\sigma^4 - \frac{15}{M^2+2}a^2 + \frac{45M^2}{N(M^2+1)(M^2+2)} = 0 \tag{26}$$

The positive solution of (26) is given by:

$$a(M,N) = \sqrt{\frac{15}{2(M^2+2)}\left[1 - \sqrt{\frac{4M(M^2+2)}{5N(M^2-1)}}\right]} \tag{27}$$

2) Principle of the recursive exponential fitting test: With the assumption of p decorrelated or partly correlated raypaths, the recursive EFT is mainly based on the comparison between the profile of ordered eigenvalues of the observation covariance matrix and the theoretical profile of the ordered noise eigenvalues. A break point occurs when signal eigenvalue appears. The general test strategy is demonstrated by Figure 2. , where two eigenvalues corresponding to raypaths are contained in the profile of the observable eigenvalues. When the eigenvalue corresponding to a raypath appears, a gap makes the profile of recorded eigenvalue break from the EFT profile.

The recursive test is started from $P = 1$. Assuming the smallest P eigenvalues are noise eigenvalues, the previous eigenvalue λ_{M-P} is tested to determine if it corresponds to noise or to a raypath. For each value of P, the test is performed by two steps:

In the first step, we predict the value of λ_{M-P} according to the exponential model, as in (19):

$$\hat{\lambda}_{M-P} = (P+1)J_{P+1}\hat{\sigma}^2 \tag{28}$$

where:

$$J_{P+1} = \frac{1 - r_{P+1}}{1 - r_{P+1}^{P+1}} \tag{29}$$

$$\hat{\sigma}^2 = \frac{1}{P+1}\sum_{i=0}^{P}\lambda_i \tag{30}$$

The prediction equation is obtained by combination of (28), (29) and (30):

$$\hat{\lambda}_{M-P} = J_{P+1}\sum_{i=0}^{P}\lambda_{M-i} \tag{31}$$

r_{P+1} is calculated by first getting a using (27) and then using the relationship $r = e^{-2a}$, where $(P+1)$ should be used instead of M.

In the second step, two hypotheses are defined as follows:

- H_{P+1}: λ_{M-P} is an eigenvalue corresponding to noise.

- $\overline{H}_{P+1}$: λ_{M-P} is an eigenvalue corresponding to a raypath.

To decide between these two hypotheses, the absolute errors of λ_{M-P} and $\hat{\lambda}_{M-P}$ are calculated and then compared with a threshold η_P. That is:

$$H_{P+1} : \left|\lambda_{M-P} - \hat{\lambda}_{M-P}\right| \leq \eta_P \tag{32}$$

$$\overline{H}_{P+1} : \left|\lambda_{M-P} - \hat{\lambda}_{M-P}\right| > \eta_P \tag{33}$$

If the absolute error of a certain value P is smaller than the related threshold, P is reset to $P+1$ and the test is repeated until $P = M-1$; otherwise, the recursive process is stopped with the detection result of $p = M - P$. Finally, we use the empirical distribution of the noise-only eigenvalue profile to find a suitable threshold. For instance, 10, 000 realizations are generated for $N = 15$ samples as well as an array of $M = 15$ sensors. Merely eight realizations are displayed for a clear explanation in Figure 1a. The mean profile of the ordered noise eigenvalue can be computed and it is represented by the middle curve. For each eigen index, there exist the largest noise eigenvalue and the smallest one. Half of the distance between them can be taken as the threshold η.

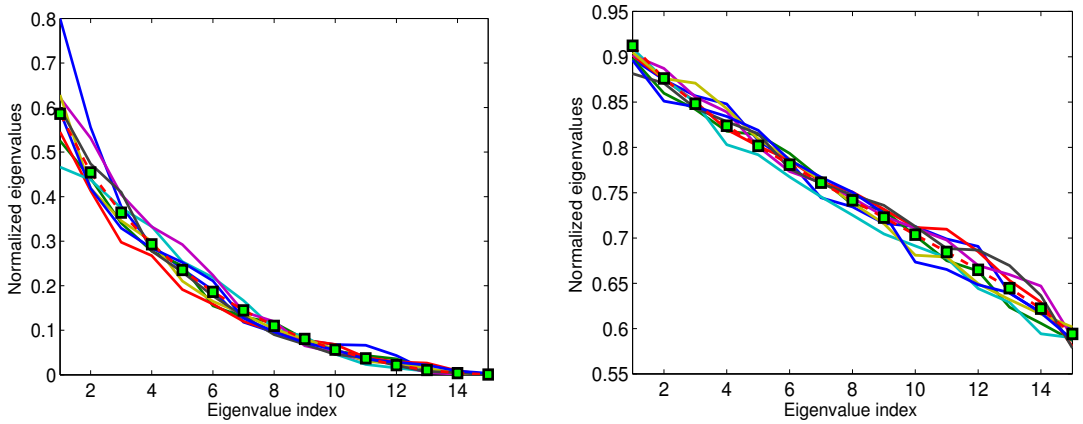

(a) (b)

Fig. 1. Profile of ordered noise eigenvalues for eight realizations (a) Profile of ordered noise eigenvalues estimated by 15 samples. (b) Profile of ordered noise eigenvalues estimated by 1025 samples.

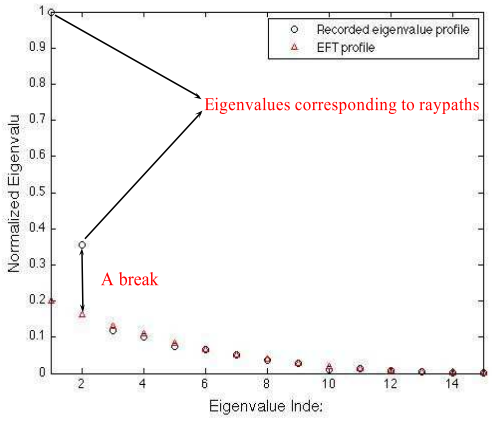

Fig. 2. Profiles of eigenvalue with two eigenvalues corresponding to raypaths. When the eigenvalue corresponding to a raypath appears, there is a break exists between the profile of EFT and the profile of recorded eigenvalues.

IV. Simulations

In this section, we illustrate the performance of EFT with simulation data. The simulation is composed of two groups of experiments. In the first group, we test the general performance of EFT for various SNRs. In the second group, the performance of EFT is addressed when the raypaths are very close.

A. Performance for various signal-to-noise ratios

For various SNRs and different number of samples, six experiments are carried out in the first group of experiments. In these experiments, five coherent raypaths arrive on 15 sensors. As the noise is added to the synthetic received signals, they could be considered as being partly correlated. As an illustration, two figures (Fig. 3 and Fig. 4) respectively plot the received raypaths and ordered eigenvalue profile for a specific SNR and number of samples. These eigenvalues are normalized by the largest one in each case. As comparative methods, the AIC and the MDL are also applied to these experiments. Considering the asymptotically consistent property of the AIC and the MDL, we chose $N = 1025$, which is much larger than the number of sensors. In this case, the AIC and the MDL still overestimate the number of raypaths. The possibility of overestimation or underestimation mainly depends on the distribution of the dispersed eigenvalue. This obeys the qualitative results in [18]. For a fixed number of samples, over-modeling becomes

more likely for the increasing of the noise eigenvalue dispersion. For a fixed dispersion, over-modeling becomes more likely for increasing the number of data samples. Under-modeling might happen in cases where the signal eigenvalues are not well separated from the noise eigenvalues and the noise eigenvalues are clustered sufficiently closely. The results are shown in Table 1. The detection results for the case of $N = 15$ imply that the EFT can detect relatively correctly for moderate or high SNRs. For the example of SNR= 5 dB, because of the correlation between raypaths and noise, EFT tends to overestimate. Obviously, the AIC and MDL cannot correctly detect the number of raypaths for short-length samples on account of asymptotically consistent performance.

SNR (dB)	AIC ($N = 1025$)	MDL ($N = 1025$)	EFT ($N = 15$)
20	14	14	5
10	14	14	5
5	14	12	11

TABLE I

NUMBER OF RAYPATHS DETECTED BY THE AIC, MDL AND EFT IN THE FIRST GROUP OF EXPERIMENTS (THE REAL NUMBER OF RAYPATHS $p = 5$)

B. Performance for close raypaths

To fully illustrate the performance of our algorithm when raypaths arrive more closely together, two experiments (SNR= 20 dB) for $N = 1025$ and $N = 15$ are performed. In these experiments, the difference is not only that the first two raypaths are closer than the examples in the first group of experiments but also the third raypath crosses the first two because of the negative arrival angle (shown in Fig.5a.). The detection results are shown in Table II. EFT still correctly detects while the AIC and MDL overestimate caused by the same reason in the discussion in Part A of Section IV. Figure. 5b, c illustrates the profiles of the ordered eigenvalue for $N = 1025$ and $N = 15$, respectively.

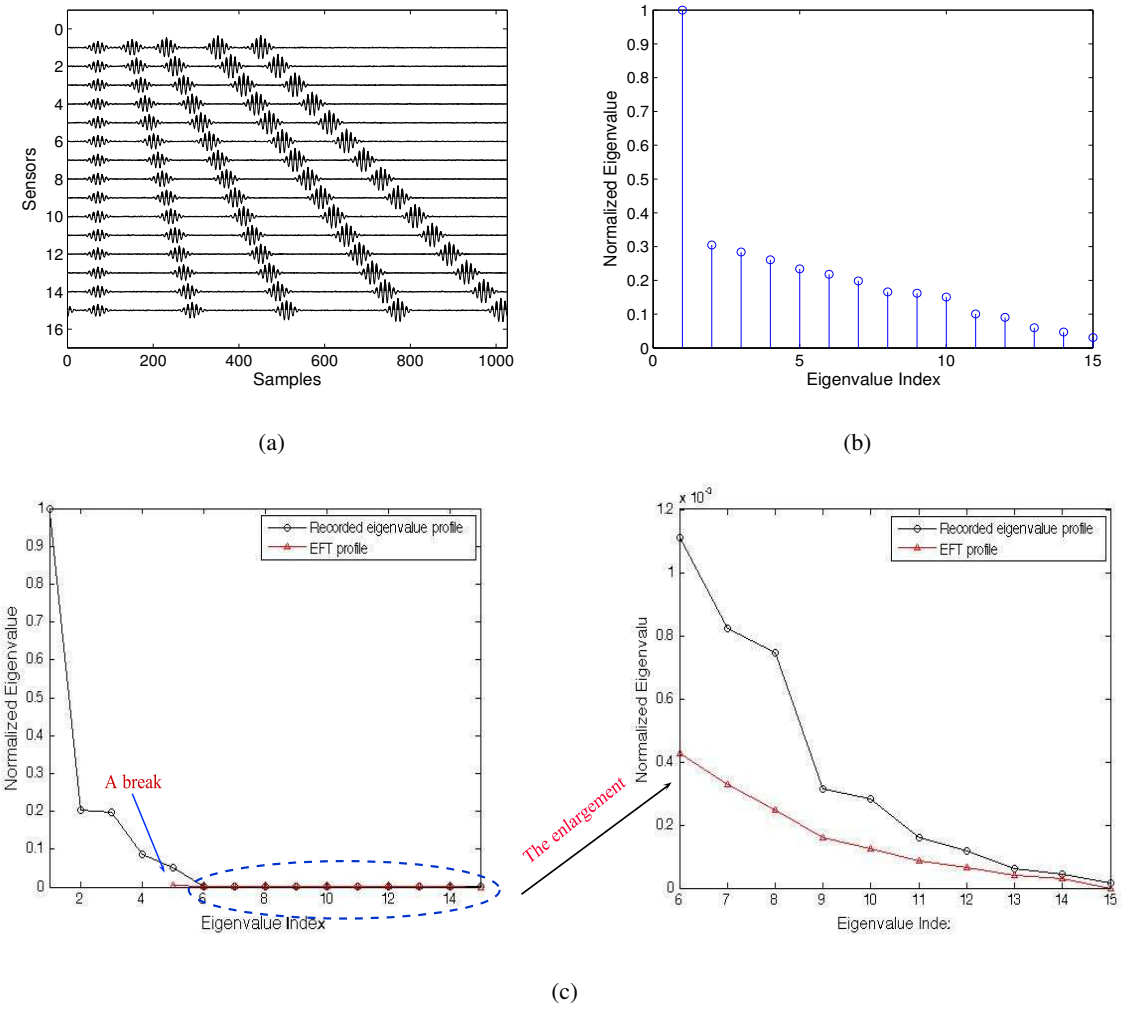

Fig. 3. Profile of the ordered eigenvalues in the first group of experiments when SNR = 20 dB (a) The received signals on 15 sensors. (b) Profile of ordered eigenvalues estimated by 1025 samples. (c) Detection with EFT (the first group of experiments when SNR = 20 dB)

SNR (dB)	AIC ($N = 1025$)	MDL ($N = 1025$)	EFT ($N = 15$)
20	14	14	5

TABLE II

NUMBER OF RAYPATHS DETECTED BY THE AIC, MDL AND EFT IN THE SECOND GROUP OF EXPERIMENTS (THE REAL NUMBER OF RAYPATHS $p = 5$)

V. THE SMALL-SCALE EXPERIMENT

A. *the noise-whitening process*

As noted before, EFT is based on the assumption of white Gaussion noise. Conversely, in a practical environment there is colored noise. The interference of colored noise can be reduced

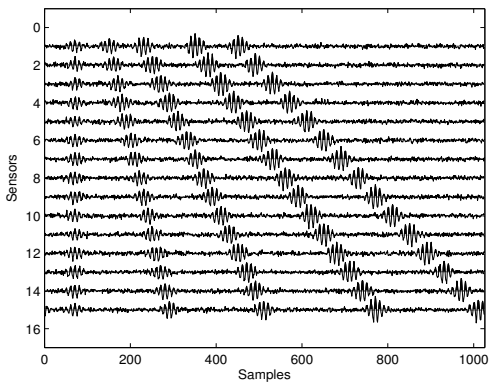

(a)

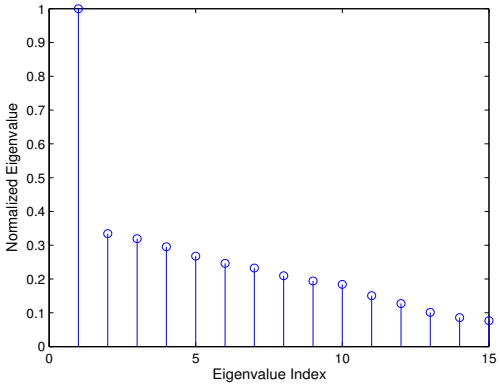

(b)

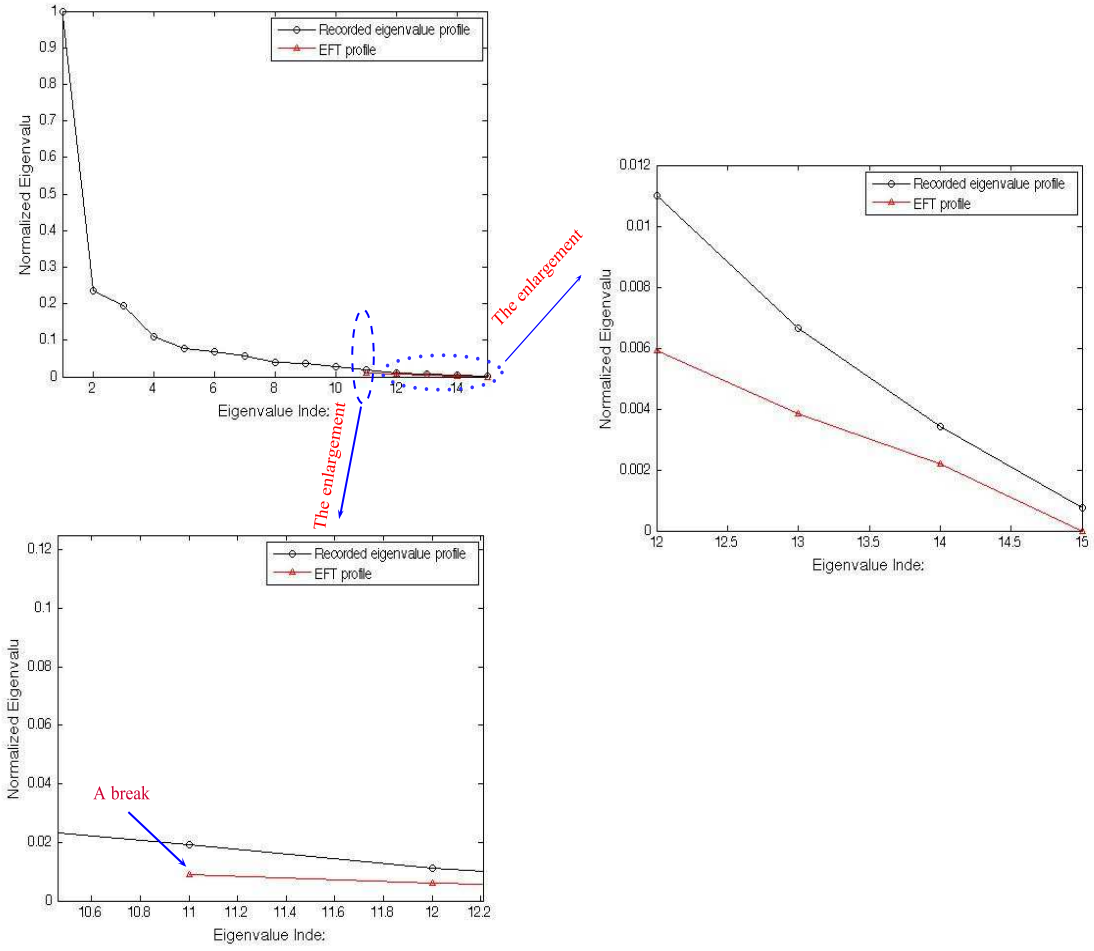

(c)

Fig. 4. Profile of the ordered eigenvalues in the first group of experiments when SNR = 5 dB (a) The received signals on 15 sensors. (b) Profile of the ordered eigenvalues estimated by 1025 samples. (c) Detection with EFT (the first group of experiments when SNR = 5 dB)

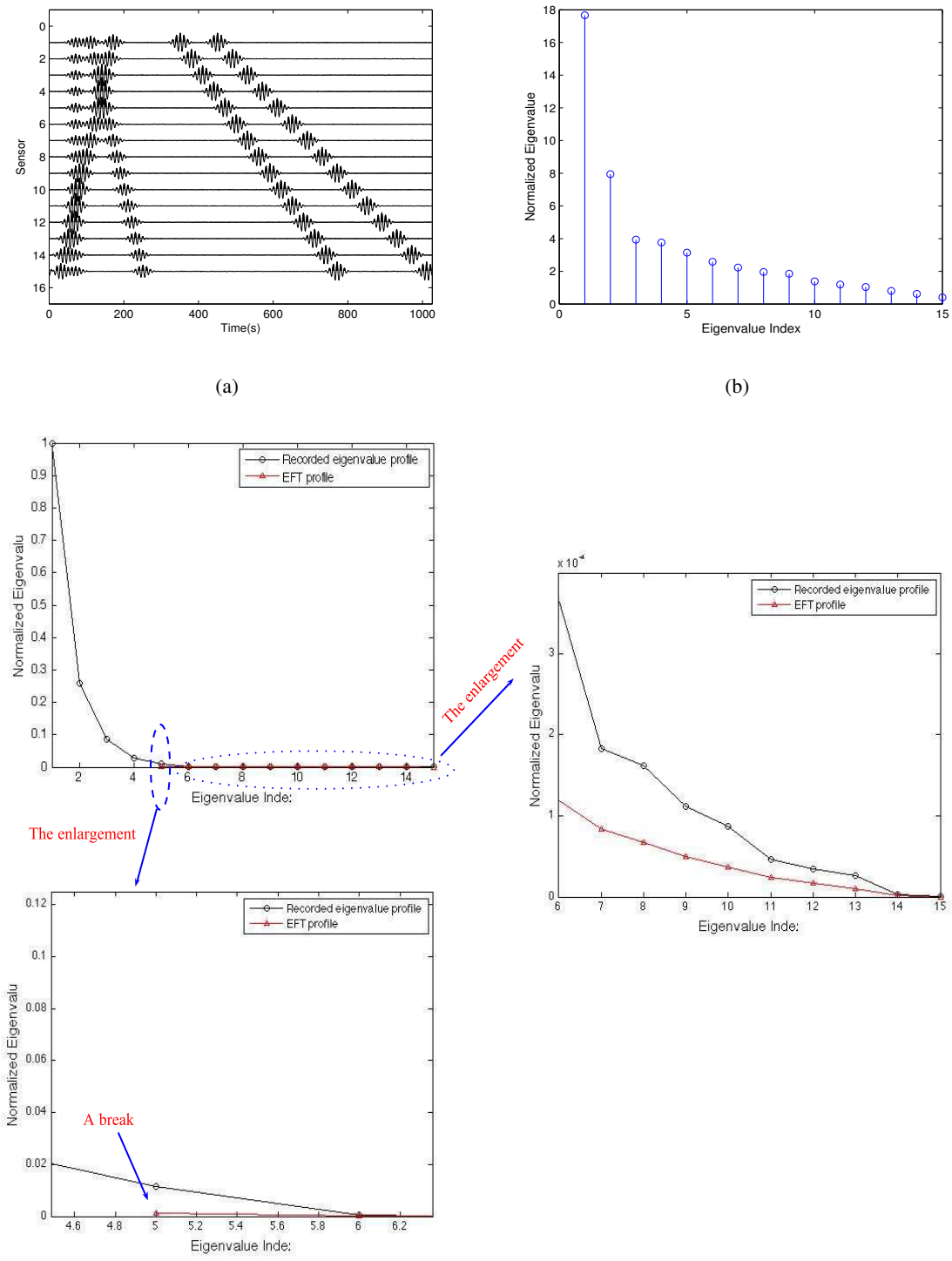

Fig. 5. Profile of the ordered eigenvalues in the second group of experiments when SNR = 20 dB (a) The received signals on 15 sensors. (b) Profile of the ordered eigenvalues estimated by 1025 samples. (c) Detection with EFT (the second group of experiments when SNR = 20 dB)

if a noise-whitening process is included. Several methods can be used to estimate the noise covariance matrix. Here, we only discuss the residual analysis method proposed by Roger [37]. The noise estimation is made simply through the inverse of its covariance matrix, which is first used to modify the principal components transform with noise adjustment [37] [38]. Then, the noise subspace projection based on the residual method is developed to estimate the number of hidden nodes for a radial basis function neural network [39] and to determinate the intrinsic dimensionality of hyperspectral imagery [40].

Exploiting the signal model in Section II, the observation covariance matrix $\mathbf{R}x$ is decomposed as:

$$\mathbf{R}_x = \mathbf{D}_R \mathbf{E}_R \mathbf{D}_R \tag{34}$$

where $\mathbf{D}_R$ is a diagonal matrix of standard deviations and that is given by $\mathbf{D}_R = diag\{\sigma_1, \sigma_2, \ldots, \sigma_M\}$ with $\{\sigma_l^2\}_{m=l}^{M}$ being diagonal elements of $\mathbf{R}_x$, and $\mathbf{E}_R$, which is represented by (35), has 1 on its principal diagonal and its other terms are the correlation coefficients between sensors.

$$\mathbf{E}_R = \begin{pmatrix} 1 & \rho_{12} & \rho_{13} & \cdots & \rho_{1M} \\ \rho_{21} & 1 & \rho_{23} & \cdots & \rho_{2M} \\ \rho_{31} & \rho_{32} & \ddots & \ddots & \vdots \\ \vdots & \vdots & \ddots & \ddots & \rho_{(M-1)M} \\ \rho_{M1} & \rho_{M2} & \cdots & \rho_{M(M-1)} & 1 \end{pmatrix} \tag{35}$$

Specifically, $\rho_{p,q}$ being the correlation coefficient at the (p, q)th entry of $\mathbf{R}_x$ and $p \neq q$.

In analogy with (34), the similar decomposition of the inverse matrix of $\mathbf{R}_x$ can be obtained as follows:

$$\mathbf{R}_x^{-1} = \mathbf{D}_{R^{-1}} \mathbf{E}_{R^{-1}} \mathbf{D}_{R^{-1}} \tag{36}$$

where $\mathbf{D}_{R^{-1}}$ is a diagonal matrix given by $\mathbf{D}_{R^{-1}} = diag\{\varsigma_1, \varsigma_2, \cdots, \varsigma_M\}$ with $\{\varsigma_l^2\}_{m=1}^{M}$ being

the values in the diagonal of $\mathbf{R}_x^{-1}$ and

$$\mathbf{E}_{R^{-1}} = \begin{pmatrix} 1 & \xi_{12} & \xi_{13} & \cdots & \xi_{1M} \\ \xi_{21} & 1 & \xi_{23} & \cdots & \xi_{2M} \\ \xi_{31} & \xi_{32} & \ddots & \ddots & \vdots \\ \vdots & \vdots & \ddots & \ddots & \xi_{(M-1)M} \\ \xi_{M1} & \xi_{M2} & \cdots & \xi_{M(M-1)} & 1 \end{pmatrix} \tag{37}$$

with $\xi_{p,q}$ being the correlation coefficient at the (p,q)th entry of $\mathbf{R}_x^{-1}$ and $p \neq q$. Referring to statistical theory and multiple linear regression [41] [42], the degree of correlation of the received signal of the mth sensor on the other $M-1$ sensor can be described by the multiple correlation coefficient r_{M-m}^2. This linear relation explains the r_{M-m}^2 proportion of received signal is the variance corresponding to raypaths. The residual variance is $\sigma_m^2(1-r_{M-m}^2)$. Further, it turns out that [41] [42] the ς_m is the reciprocal of the residual standard deviation. Thus, (38) is obtained:

$$\varsigma_m = \sigma_m^{-1}(1-r_{M-m}^2)^{-\frac{1}{2}} = \frac{1}{\sqrt{\sigma_m^2(1-r_{M-m}^2)}} \tag{38}$$

The major advantage of using ς_m over σ_m is that ς_m removes its correlation on other ς_k for $k \neq m$. Therefore, the noise covariance matrix $\mathbf{R}_n$ can be estimated by: $\mathbf{R}_n = diag\left\{1/\varsigma_1^2, 1/\varsigma_2^2, \ldots, 1/\varsigma_M^2\right\}$.

Based on the above discussion, the sample covariance matrix $\mathbf{R}_x$ can be whitened using the estimated noise covariance $\mathbf{R}_n$:

$$\mathbf{R}_w = \mathbf{R}_n^{-1/2}\mathbf{R}_x\mathbf{R}_n^{-1/2} \tag{39}$$

B. The small-scale experiment

A small-scale experiment is discussed in this part, so that we can further illustrate the performance of our methods. The experimental setup is illustrated in Figure. 6. The principle on which these experiments are based is as follows: if the frequency of signals is multiplied by a factor and the spatial distances are divided by the same factor, the physical phenomena occurring in the environment remain the same. This promotes a reduced cost and provides a totally controlled experiment. The experiments presented here were performed at the ISTerre (Institut des Sciences de la Terre) in an ultrasonic tank which was developed by P. Roux. In

this tank, a waveguide of 5-10 m in depth and 1.0-1.5 m in length was constructed. A steel bar acts as the bottom, which is very reflective and perfectly flat. In particular, a sensor is set at 0.0263 m in depth range as the source. A vertical array composed of 64 sensors is used as a receiver. The depth of the first receiver is $3.55 \times 10^{-3} m$. The interval of two adjacent receivers is 0.75×10^{-3}m. The distance between the source and the reference receiver is 1.1437 m and the source signal has 1 MHz frequency bandwidth with a central frequency of 1.2 MHz. Figure. 7a shows that the first 5, 000 points in the time domain of received signals with sampling frequency $F_e = 50MHz$.

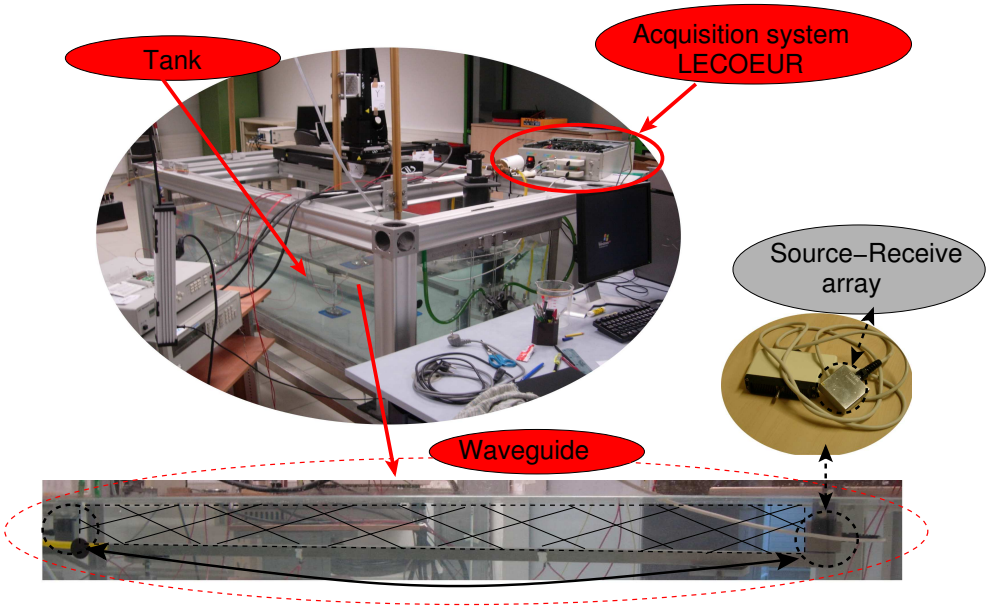

Fig. 6. Experimental setup of small-scale experiment at the ISTerre

To satisfy the criterion of short-length samples, 64 samples of a recorded signal were chosen for analysis. To evaluate the effectiveness of EFT and NWEFT, the separation result of the beamforming is provided in Figure. 7b. It matches by the theoretical locations denoted in the form of the crosses. The eigenvalue profile is shown by Figure. 7c. EFT detects 6 raypaths. Meanwhile, the detection result of NWEFT is 6. Compared to the reference value 7 in Fig. 7 (b), these methods can be taken as being acceptable. Based on these experiments, we can see that the overestimation caused by the correlation between the raypaths and noise, especially when the SNR is relatively low. Underestimation is caused by the correlations between the raypaths.

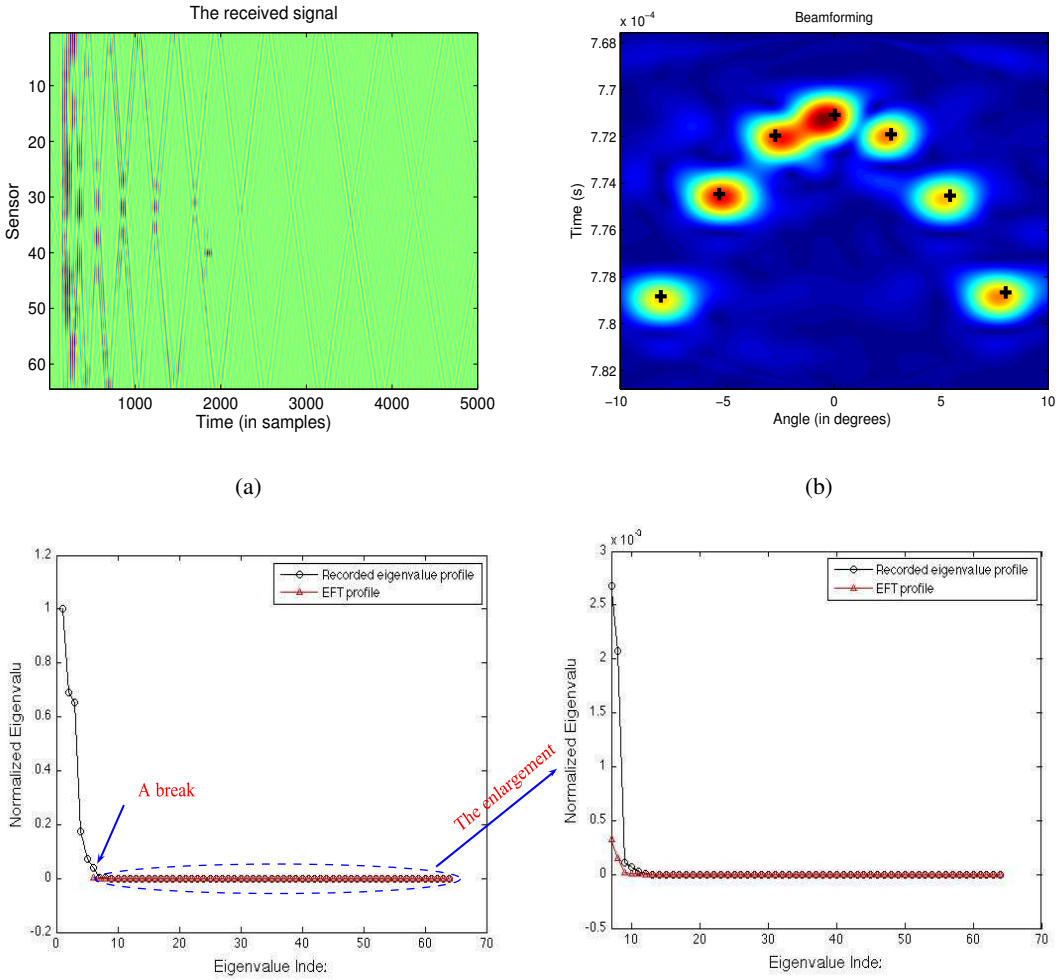

Fig. 7. (a) The received signals on 64 sensors for 5000 samples. (b) Separation result of beamforming with theoretical locations for 64 samples. This provides a reference value for checking the detection results of the proposed method. (c) Detection with EFT (real data obtained from the small-scale experiment).

we have applied AIC and MDL using 760 samples on the same set of real data. Their detection results are both equal to 63.

VI. Conclusions

In this paper, a NWEFT method is proposed to automatically detect the number of raypaths in a shallow-water waveguide. As the AIC and the MDL are confined by the duration of the received signal, they fail to correctly detect the number of raypaths. In contrast, the proposed method can determine the number of raypaths using short-length samples. Due to the noise whitening

process, this can be applied to the real application environment. In future, the detection method to consider quantitatively the influence of correlations between raypaths as well as correlations between raypaths and noise, should be studied further. This method can also be extended to medium-length samples.

VII. ACKNOWLEDGMENTS

The authors would like to thank Associate Editor Dr. Gopu Potty and anonymous reviewers for their constructive suggestions and invaluable remarks that improved the presentation of the paper.

REFERENCES

[1] W. Munk, P. Worcester, and C. Wunsch, Ocean Acoustic Tomography, *Cambridge monographs on mechanics, Cambridge*, 1995.

[2] X. Dmoulin, Y. Stphan, S. Jesus, E. Ferreira, and M. Porter, "Intimate96: A shallow water tomography experiment devoted to the study of internal tide," *China Ocean Press: Shallow Water Acoust.* , vol. 130, 485490, 1997.

[3] P. Roux, B.D. Cornuelle, W. A. Kuperman, and W. S. Hodgkiss, "The structure of raylike arrivals in a shallow-water waveguide," *J. Acoust. Soc. Ameri.*, vol. 124, pp. 3430-3439, 2008.

[4] I. Iturbe, P. Roux, B. Nicolas, and J.I. Mars, "Ocean acoustic tomography using a double-beamforming algorithm," *J. Acoust. Soc. Ameri.*, vol. 123, no. 5, pp. 3912-3917, 2008.

[5] I. Iturbe, P. Roux, B. Nicolas, J. Virieux and J.I. Mars, "Shallow-water acoustic tomography performed from a double-beamforming algorithm: simulation results," *IEEE J. Oceanic. Eng.* , vol. 34, no. 2, pp. 140-149, 2009.

[6] P. Roux, I. Iturbe, B. Nicolas, J. Virieux and J.I. Mars, "Travel-time tomography in shallow water: Experimental demonstration at an ultrasonic scale," *J. Acoust. Soc. Ameri.*, vol. 130, pp. 1232, 2011.

[7] P. Pignot and N.R. Chapman, "Tomographic inversion of geoacoustic properties in a range-dependent shallow-water environment," *J. Acoust. Soc. Ameri.*, vol. 110, pp. 1338-1348, 2001.

[8] Y.M. Jiang, N.R. Chapman and P. Gerstoft, "Short range travel time geoacoustic inversion with vertical line array," *J. Acoust. Soc. Ameri.*, vol. 124, pp. EL135-EL140, 2008.

[9] Z. H. Michalopoulou and M. Picarelli, "Gibbs sampling for time-delay-and amplitude estimation in underwater acoustics," *J. Acoust. Soc. Ameri.*, vol. 117, pp. 799-808, 2005.

[10] Z. H. Michalopoulou and X. Ma, "Source localization in the Haro Strait primer experiment using arrival time estimation and linearization," *J. Acoust. Soc. Ameri.*, vol. 118, pp. 2924-2933, 2005.

[11] L. Jiang, F. Aulanier, G. Touzé, B. Nicolas and J. I. Mars, "Raypath Separation with High Resolution Processing," *in Proceeding of Oceans 11 IEEE Santander, Spain*, Jun. 6-9, 2011.

[12] M. Wax and T. Kailath, "Detection of signals by information theoretic criteria," *IEEE Trans. Acoust. Speech Signal Process.*, vol. 33, no. 2, pp. 387-392, 1985.

[13] H. Akaike, "Information theory and an extension of the maximum likelihood principle," *in Proceedings of 2nd Int. Symp. Inform. Theory, suppl. Problems of Control and Inform. Theory*, pp. 267-281, 1973.

[14] R. J. Muirhead, Aspects of multivariate statistical theory, *Wiley Online Library*, vol. 42,1982.

[15] A. T. James, "The distribution of the latent roots of the covariance matrix," *Ann. Math. Statist.* vol. 31, pp. 151-158, 1960.

[16] A. T. James, "Zonal polynomials of the real positive definite symmetric matrices," *Ann. Math. Statist.* vol. 74 (3), pp. 456-469, 1961.

[17] W. Xu and M. Kaveh, "Analysis of the performance and sensitivity of eigendecomposition-based detectors," *IEEE Trans. Signal Process.*, vol. 43, pp. 1413-1426, 1995.

[18] A. P. Liavas and P. A. Regalia, "On the behavior of information theoretic criteria for model order selection," *IEEE Trans. Signal Process.*, vol. 49, no. 8, pp. 1689-1695, 2001.

[19] E. Fishler and H. Messer, "On the Use of Order Statistics for Improved Detection of Signals by the MDL Criterion," *IEEE Trans. Signal Process.*, vol. 48, no. 8, pp. 2242-2245, 2000.

[20] S. Valaee and Peter Kabal, "An Information Theoretic Approach to Source Enumeration in Array Signal Processing," *IEEE Trans. Signal Process.*, vol. 52, no. 5, pp. 1171-1178, 2004.

[21] J. Dettmer, S. E. Dosso and C.W. Holland, "Model selection and Bayesian inference for high-resolution seabed reflection inversion," *J. Acoust. Soc. Ameri.*, vol. 125, pp. 706-716, 2009.

[22] P. M. Djuric, "Model selection based on asymptotic Bayes theory," *in Proceedings of the Seventh SP Workshop on Statistical Signal and Array Processing,* pp. 387-392, 1994.

[23] P. M. Djuric, "A model selection rule for sinusoids in white Gaussian noise," *IEEE Trans. Signal Process.*, vol. 44, no. 2, pp. 1744-1751, 1996.

[24] M.S. Bartlett, "A note on the multiplying factors for various χ^2 approximations,", *J. Roy. Stat. SOC.*, vol. 16, no. E, pp. 296-298, 1954.

[25] D. N. Lawley, "Tests of significance of the latent roots of the covariance and correlation matrices," *Biometrica*, vol. 43, pp. 128-136, 1956.

[26] H. Gu, "Estimating the Number of Signals and Signal Resolution," *IEEE Trans. Signal Process.*, vol. 46, no. 8, pp. 2267-2270, 1998.

[27] P. Stoica, Y. Seln, and J. Li, "On Information Criteria and the Generalized Likelihood Ratio Test of Model Order Selection," *IEEE Trans. Signal Process.*, vol. 11, no. 10, pp. 794-797, 2004.

[28] A. A. Shah and D. W. Tufts, "Determination of the Dimension of a Signal Subspace from Short Data Records," *IEEE Trans. Signal Process.*, vol. 42, no. 9, pp. 2531-2535, 1994.

[29] J. Grouffaud, P. Larzabal, and H. Clergeot, "Some properties of ordered eigenvalues of a Wishart matrix: application in detection test and model order selection," *ICASSP* vol. 5, pp. 2463-2466, 1996.

[30] A. Quinlan, J.-P. Barbot, and P. Larzabal, "Automatic determination of the number of targets present when using the time reversal operator," *J. Acoust. Soc. Ameri.* vol. 119, no. 4 ,pp. 2220-2225, 2006.

[31] R. R. Nadakuditi and A. Edelman, "Sample Eigenvalue Based Detection of High-Dimensional Signals in White Noise Using Relatively Few Samples," *IEEE Trans. Signal Process.* , vol. 56, no. 7, pp. 2625-2638, 2008.

[32] H. Akaike, "A new look at the statistical model identification," *IEEE Trans. Automat. Control* vol. AC-19, pp. 716-723, 1974.

[33] G. Schwarz, "Estimating the dimension of a model," *Ann. Stat.*, vol. 6, pp. 461-464, 1978.

[34] J. Rissanen, "Modeling by shortest data description," *Automatica*, vol. 14, pp. 465-471, 1978.

[35] N. L. Johnson and S. Kotz, "Distributions in Statistics: Continuous Multivariate Distributions," *chapter 38-39, John Wiley Sons, New York, NY, USA*, 1972.

[36] P. R. Krishnaiah and F. J. Schurmann, "On the evaluation of some distribution that arise in simultaneous tests of the equality of the latents roots of the covariance matrix," *J. Multivariate Analysis* vol. 4, pp. 265-282, 1974.

[37] R. E. Roger, "Principal components transform with simple, automatic noise adjustment," *Int. J. Remote Sens.*, vol. 17, no. 14, pp. 2719-2727, 1996.

[38] R. E. Roger and J. F. Arnold, "Reliably estimating the noise in AVIRIS hyperspectral imagers," *Int. J. Remote Sens.*, vol. 17, no. 10, pp. 1951-1962, 1996.

[39] Q. Du and C.-I Chang, "An interference rejection-based radial basis function neural network approach to hyperspectral image classification," *in Proc. Int. Joint Conf. Neural Networks, Washington, DC,* pp. 2698-2703, Jul., 1999.

[40] C.-I. Chang and Q. Du, "Estimation of number of spectrally distinct signal sources in hyperspectral imagery,", *IEEE Trans. Geosci. Remote Sensing,* vol. 42, no. 3, pp. 608-619, 2004.

[41] A. M. Kshirsagar, "Multivariate Analysis," *Marcel Deker, New York*, 1972.

[42] R. J. Harris, A Primer of Multivariate Statitics, 2nd edn, *Academic Press, Orlando*, 1985.